Bioorg. Med. Chem. 94 (2023) 117481

Contents lists available at ScienceDirect

Bioorganic & Medicinal Chemistry

journal homepage: www.elsevier.com/locate/bmc

# Designing peptide amphiphiles as novel antibacterials and antibiotic adjuvants against gram-negative bacteria

Huihua Xing [a], Vanessa Loya-Perez [b], Joshua Franzen [c], Paul W. Denton [c], Martin Conda-Sheridan [a], Nathalia Rodrigues de Almeida [b,*,1]

[a] Department of Pharmaceutical Sciences, College of Pharmacy, University of Nebraska Medical Center, Omaha, NE 68198, United States
[b] Department of Chemistry, University of Nebraska Omaha, Omaha, NE 68182, United States
[c] Department of Biology, University of Nebraska Omaha, Omaha, NE 68182, United States

A B S T R A C T

Gram-negative strains are intrinsically resistant to most antibiotics due to the robust and impermeable characteristic of their outer membrane. Self-assembling cationic peptide amphiphiles (PAs) have the ability to disrupt bacteria membranes, constituting an excellent antibacterial alternative to small molecule drugs that can be used alone or as antibiotic adjuvants to overcome bacteria resistance. PA1 ($C_{16}$KHKHK), self-assembled into micelles, which exhibited low antibacterial activity against all strains tested, and showed strong synergistic antibacterial activity in combination with Vancomycin with a Fractional Inhibitory Concentration index (FIC*i*) of 0.15 against *E. coli*. The molecules, PA2 ($C_{16}$KRKR) and PA3 ($C_{16}$AAAKRKR), also self-assembled into micelles, displayed a broad-spectrum antibacterial activity against all strains tested, and low susceptibility to resistance development over 21 days. Finally, PA1, PA 2 and PA3 displayed low cytotoxicity against mammalian cells, and PA2 showed a potent antibacterial activity and low toxicity in preliminary *in vivo* models using *G. mellonella*. The results show that PAs are a great platform for the future development of effective antibiotics to slow down the antibiotic resistance and can act as antibiotic adjuvants with synergistic mechanism of action, which can be repurposed for use with existing antibiotics commonly used to treat gram-positive bacteria to treat infections caused by gram-negative bacteria.

## 1. Introduction

Antibiotic resistance still remains one of the greatest health concerns globally, and it has become an even more serious threat following the COVID-19 pandemic. According to a CDC report from 2022[1], the COVID-19 pandemic caused a huge impact in antibiotic resistance due to a lack of data reporting for 9 pathogenic threats and an increased number of antibiotic prescriptions for patients (even though antibiotics are not effective for viruses). Out of the 18 most serious antibiotic-resistant threats listed, 10 are gram-negative strains.[2] For example, the available data show an increase of 78% of Carbapenem-resistant *Acinetobacter* infections, 35% of Carbapenem-resistant *Enterobacteriaceae*, 14% of Vancomycin-resistant *Enterococci*, and 13% of Methicillin-resistant *Staphylococcus aureus* compared to the 2019 CDC data.[1] This problem is exacerbated by the fact that many large pharmaceutical companies are no longer investing as much in antibiotic R&D.[3] According to the latest WHO report, only 2 out of 27 antibiotics under development against WHO bacterial priority pathogens meet at least one criteria of innovation or are active against multidrug resistant gram-negative bacteria. To make this situation even more concerning, nearly 80% of the newly approved antibiotics belong to the existing class of antibiotics which bacteria already has developed resistance.[4] Thus, there is an urgent need for alternative strategies to treat bacterial infections.

Gram-negative bacteria are protected from external agents by the presence of the outer membrane (OM) barrier and efflux mechanism. The outer membrane is an asymmetrical lipid bilayer composed of highly packed lipopolysaccharides (LPS) and negatively charged phospholipids which form a robust barrier that is effective at preventing the accumulation of drugs. Antibiotics with activity against gram-negative bacteria are (essentially) limited to small and hydrophilic drugs with MW lower than 600 Da that can cross the membrane via porins.[5–7] Moreover, these membrane characteristics make gram-negative bacteria intrinsically resistant to antibiotics[8], limiting the options available to treat these pathogens. In addition to innate resistance, bacteria can also develop resistance against antibiotics via different mechanisms. One of the approaches to overcome this problem includes chemical perturbation or disruption of the outer membrane, allowing the accumulation of antibiotics traditionally active against gram-positive bacteria to

* Corresponding author.
*E-mail address:* nalmeida@trinity.edu (N. Rodrigues de Almeida).
[1] Current address: Department of Chemistry, Trinity University, San Antonio, TX 78212, United States.

https://doi.org/10.1016/j.bmc.2023.117481
Received 28 June 2023; Received in revised form 15 September 2023; Accepted 18 September 2023
Available online 20 September 2023

permeate inside gram-negative bacteria.[9,10].

For example, combinations of pentamidine, an antiprotozoal agent used to treat pneumocystis pneumonia, trypanosomiasis, and leishmaniosis, with antibiotics such as minocycline, linezolid, valnemulin, and nadifloxacin have shown enhanced activity against multidrug-resistant bacteria including *Escherichia coli*, *Acinetobacter baumannii*, *Pseudomonas aeruginosa*, *Klebsiella pneumoniae*.[11] Pentamidine also potentialized novobiocin in a dose-dependent manner against colistin-resistant *A. baumannii* in a murine model.[10] However, the toxicity of pentamidine is a big concern. Patients treated with pentamidine often develop nephrotoxicity, hypotension, hypoglycemia, hepatic dysfunction, QT prolongation and leucopenia.[12,13].

There are also some literature reports showing an increase in efficacy and slow development of resistance when antibiotics are combined with molecules that potentiates their activity.[15–21] For example, cyclic amphiphilic peptides combined with tetracycline, tobramycin, clindamycin, kanamycin, levofloxacin, polymyxin B, metronidazole, and vancomycin have been shown to display synergistic antibacterial activity against *S. aureus, P. aeruginosa, E. coli and K. pneumoniae*.[14] Antimicrobial peptides have been reported to synergize with vancomycin against gram-negative bacteria.[15] Peptidomimetics[16], cell-penetrating peptides[17], small molecule,[18] and synthetic polymers[19,20] also have been reported to enhance the antibacterial activity of existing antibiotics against multidrug-resistant pathogens. These membrane-active compounds are often cationic and/or amphiphilic, and the biggest limitation is their toxicity[12] (ability to disrupt host cell membranes), and poor pharmacokinetics properties including low availability and metabolic stability.[21].

Self-assembling Peptide Amphiphiles (PAs) make an excellent candidate as novel antibiotics and antibiotic adjuvants because they are biocompatible, are less likely to be immunogenic[22] due to use of proteinogenic amino acids, have structural similarities to endogenous peptides, and they are likely to have increased metabolic stability (when compared to linear antimicrobial peptides) due to the presence of an hydrophobic tail and their ability to form nanostructures.[23–25] Still, one of the biggest challenges of antibacterial PAs is the cytotoxicity against mammalian cells and red blood cells. Cytotoxicity toward these cells have been linked to the overall hydrophobicity and the length of the alkyl tail,[26,27] but the use of drug combinations is a great approach to overcome the cytotoxicity of these lipopeptides due to significantly lower concentrations needed for antibacterial activity.

Aiming to improve specificity of these PAs as antibacterial and antibacterial adjuvants, we designed and synthesized a small library of novel PAs with hexadecanoyl ($C_{16}$) hydrophobic tails with various basic amino acids (positively charged) residues to target bacteria membranes. According to our previous report, $C_{16}$ tail has showed better selectivity against bacterial strains.[27] We also designed PAs containing octadecanoyl ($C_{18}$) hydrophobic tails with shorter side chain basic amino acids to decrease the overall hydrophobicity of the PA molecules. We determined the morphology of the self-assembled nanostructures by Transmission Electron Microscopy (TEM). To address whether PAs present antibacterial activity and would synergistically enhance efficacy and availability of antibiotics to reduce bacteria resistance and cytotoxicity, we conducted antibacterial assays to determine Minimum Inhibitory Concentration (MIC), checkerboard assays to study synergy between PAs and antibiotics to determine FIC*i*, Propidium Iodide (PI) uptake to study inner membrane permeability, and bacteria resistance assays to study the antibacterial activity of the assemblies alone and in combination with other antibiotics. We also studied the cytotoxicity of the PAs in HEK-293 and red blood cells and performed a preliminary investigation of *in vivo* antibacterial efficacy using *G. mellonella*.

## 2. Materials and methods

### 2.1. Synthesis of peptide amphiphiles (PAs)

The PAs were synthesized using standard Fmoc Solid Phase Peptide Synthesis (SPPS) according to procedures published in a previous report (Supporting Information (SI1).[28] PAs were prepared either manually or using a Alstra Biotage microwave peptide synthesizer in a 0.3 mmol scale using rink amide resin (AAPPTEC). The Fmoc-Rink Amide MBHA Resin was purchased from AAPPTEC (Louisville, KY) and the FMOC L-amino acids and coupling agents including N,N'-Diisopropylcarbodiimide (DIC) and N,N,N′,N′-Tetramethyl-O-(1H-benzotriazol-1-yl)uronium hexafluorophosphate (HBTU) were purchased from AAPPTEC and Novabiochem (MilliporeSigma). Other solvents and reagents including dichloromethane (DCM), dimethylformamide (DMF), N,N-Diisopropylethylamine (DIPEA)and 4-methylpiperidine were purchased from Fisher Chemicals (ThermoFisher Scientific). The chemical structure of the molecules was confirmed by MALDI-TOF-MS (SmartFlex bench top MALDI-TOF MS Bruker and Bruker's Autoflex maX MALDI-TOF/TOF). The products were purified using a preparative reverse phase high-performance liquid chromatography (RP-HPLC; Agilent) in a C18 column as the stationary phase of 5 μm, 100 Å pore size, and 150 × 21.1 mm (Phenomenex) with a gradient of ACN/$H_2O$ (containing 0.1% of trifluoroacetic acid - TFA). The purity of the new PAs was confirmed by an analytical HPLC instrument using a C18 column at a wavelength of 220 nm with a linear gradient of ACN/$H_2O$ (0.1% TFA) from 5 to 95% for 30 min. The pH of the water solution was adjusted to 7 and then lyophilized using a Labconco FreeZone Benchtop Freeze Dryer. All PA samples were self-assembled in ultrapure water at 1 mg/mL and the pH was adjusted to 7. The solutions were heated to 70℃ for 2 h and incubated at r.t. overnight before testing.

### 2.2. Zeta potential

The PA samples were prepared at 1 mg/mL concentration, the pH was adjusted to 7 by addition of HCl or NaOH), annealed at 80 °C for 2 h, and aged overnight. Before the experiment, the PA solutions were diluted to 250 μg/mL in HPLC grade water. Zeta Potential was determined using a Zetasizer NanoZS (Malvern Instruments) at 25 °C. For bacteria assays, *S. aureus* JE2 (MRSA) and *E. coli* K12 were cultured in Muller−Hinton broth (MHB) to mid logarithmic-phase (OD. ~ 0.8). Bacteria cells were washed and resuspended in PBS to 5 × $10^7$ colony forming unit per mL (CFU/mL) and treated with PAs at 10 × MIC for 1 h before the zeta potential measurements. Polymyxin B and Daptomycin were used as standard drugs and bacteria cells without treatment were used as negative control.

### 2.3. Transmission electron microscopy (TEM)

The PAs were dissolved in HPLC grade water to give a final concentration of 2 mM and pH was adjusted to 7, which is near physiological pH. Our previous study have shown that salt concentration (lower than 1 M concentration) has a minimal effect on the morphology of similar structures in this manuscript (i.e, $C_{16}K_2$ and $C_{16}K_3$).[29] In addition, we have reported that self-assembly in different conditions (e.g. changing counter ion) has no effect on the antimicrobial activity of PAs.[27] The samples were incubated at room temperature overnight before the experiments. Approximately, 6 μL of the sample was applied onto a copper grid and allowed to absorb for 5 min, covered with a folded piece of filter paper like a tent. The excess PA was removed from the grid by inverting the forceps and touching only the edge of the grid to a clean piece of the filter paper. Then, 6 μL of the negative stain (NanoVan) was added for 30 s. The excess stain was removed, and the PAs were imaged with a FEI TEcnai G2 Spirit transmission electron microscope (120 kV), and an AMT digital imaging system.

### 2.4. Minimal Inhibitory concentration (MIC)

The MICs were determined using the broth microdilution method as previously described.[27] Bacterial cultures were made by the direct colony suspension method to $1.5 \times 10^8$ colony forming unit per mL (CFU/mL) (0.5 McFarland) and diluted in Muller−Hinton broth (MHB) to a final concentration of $\sim 10^5$ CFU/mL. A stock solution of each PA to be tested was prepared in HPLC grade water at 1 mg/mL concentration and pH was adjusted to 7. The dilutions were made in MHB (100 μL per well), in 96-well plates (Greiner, Bio-One), after that, each well was inoculated with 10 μL of bacterial cultures and plates were incubated for about 20–24 h at 37 °C. The lowest concentration of PA that inhibits bacterial growth was considered the MIC. The optical density (O.D.) was recorded using an AccuSkan, MultiSkan FC (Thermo Fisher Scientific) at 600 nm. Vancomycin and Gentamicin were used as positive controls and media was used as negative control. Samples were tested in triplicate. 1% 2,3,5-Triphenyltetrazolium chloride (TTC) solution was used to stain for easier visualization.

### 2.5. Checkerboard assay

*E. coli* K12 and *A. baumannii* clinical strain (deidentified strain collected in the clinical microbiology laboratory at Nebraska Medicine) were grown overnight to mid logarithmic phase (OD. ~ 0.8) in MHB medium and diluted in MHB to $\sim 10^5$ CFU/mL. Antibiotic synergy was determined using checkerboard broth microdilution assays with two-fold serial dilutions of antibiotics (Rifampicin and Vancomycin) across the 96-well plate (Greiner, Bio-One), (horizontal) and two-fold serial dilutions of PAs down the plates (vertical) to final volumes of 100 μL. After the serial dilutions were made, 10 μL of bacteria culture were added to each well and the plates were incubated for 20–24 h at 37 °C. The O.D. was recorded with an AccuSkan, MultiSkan FC (Thermo Fisher Scientific) at 470 nm. Fractional inhibitory concentration index (FICi) was calculated according to the following equation (equation 1):

$$FICi = \frac{MICac}{MICa} + \frac{MICbc}{MICb} = FICa + FICb$$

where *MICa* is the MIC of compound A alone; *MICac* is the MIC of compound A in combination with compound B; *MICb* is the MIC of compound B alone; *MICbc* is the MIC of compound B in combination with compound A; *FICa* is the FIC of compound A; *FICb* is the FIC of compound B. Synergy as defined as an *FICi* of $\leq 0.5$[11], Additive and indifference was defined as an FICi of 0.5–4[11] and Antagonism was defined as an *FICi* of $\geq 4$.[11].

### 2.6. Bacteria resistance studies

The resistance induction studies were performed in *S. aureus* JE2 (MRSA) and *E. coli* K12 using broth microdilution method after 21 passages following procedures described in the literature.[30,31] and the MIC values were assessed after every passage. 21 days is an appropriate time frame because of the fast cell division of bacteria. For example, others have investigated the development of bacteria resistance against antibacterial nanoparticles over periods of 5–15 days.[32] On day 1, the MIC value for the PAs was assessed using the MIC assay method described above. On day 2–21, the MIC assays for PAs and vancomycin were performed with at least 3 concentrations above and 3 concentrations below previous MIC values (1/8 MIC, 1/4 MIC, ½ MIC, MIC, 2 × MIC, 4 × MIC, and 8 × MIC). The bacteria suspension at the sub-MIC concentration from the previous day was diluted to $1.5 \times 10^8$ colony forming unit per mL (CFU/mL) (0.5 McFarland) in MHB. The bacteria culture was further diluted in MHB to a final concentration of $1.5 \times 10^5$CFU/mL and 100 μL was added into the serial-diluted assay plate containing the PAs. The plate was incubated at 37°C for 20–24 h, and1% TTC solution was used to stain for easier visualization. The MIC tests were repeated for 21 days.

### 2.7. Propidium iodide (PI) uptake

*E. coli* K12 cells were grown in MHB to the mid logarithmic-phase and the bacterial cells were separated by centrifugation at 5000 rpm for 15 min and washed twice with HyClone Dulbecco's phosphate buffered saline (PBS) solution (GE Healthcare Life Science). Bateria cells were diluted to $10^6$ CFU/mL using 5 mM HEPES buffer + glucose. Bacteria suspensions containing 2 mM of PI were incubated at 37 °C for at least 15 mins before treatment withPAs and antibiotics. In a 96-well plate, 40 μL of PAs and Vancomycin at different concentrations (1/8 MIC, 1 × MIC, and 2 × MIC) and the PA-Vancomycin drug combination (1:1 ratio of PA-Vancomycin) were added to each well. Then, 160 μL of PI-stained bacteria solution was added to each well. Polymyxin B was used as a reference drug (positive control) and cells with no antibiotic treatment were used as a negative control. The PI fluorescence was measured using a spectrofluorometer (SoftMax Pro7.1 and SpectraMax M5[e]) with excitation and emission wavelengths set at 535 nm and 615 nm, respectively.

### 2.8. Scanning electron microscopy (SEM)

*S. aureus* JE2 (MRSA) and *E. coli* K12 were grown in MHB at 37 °C and the resultant mid-log phase culture was diluted in PBS (GE Healthcare Life Science) to a final concentration of $1.5 \times 10^8$ CFU/mL. The bacteria cells were treated with PA2 at twice the MIC value and then incubated for 2 h at 37 °C. Untreated cells (with no PA added) were used as a control. After the incubation, the bacteria cells were washed three times with PBS and the samples were fixed in a solution of 2.0% (v/v) glutaraldehyde and 2% (v/v) of paraformaldehyde in phosphate buffer (0.1 M, pH 6.2) for 24 h at 4 °C. The samples were placed on glass chips coated with 0.1% poly-L lysine, allowed to adhere for 30 min and then washed three times with PBS. After fixing, samples were treated with a 1% aqueous solution of osmium tetroxide for 30 min to aid in conductivity. After that, samples were dehydrated in a graded ethanol series (50, 70, 90, 95 and 100% EtOH solutions). Then, samples were critical point dried and attached to aluminum SEM stubs with double-sided carbon tape. Silver paste was applied to increase conductivity. The following day, samples were coated with ~50 nm gold–palladium alloy in a Hummer VI Sputter Coater (Anatech USA) and imaged at 30 kV in a FEI Quanta 200 SEM operating in high vacuum mode.

### 2.9. Cytotoxicity

HEK-293 cells were cultured using ATCC protocols at 37 °C in a humidified environment with 5% $CO_2$ and passages 3–8 were used for all the experiments. The assays were carried out in sterile 96-well flat-bottomed polystyrene microtiter plates (Greiner, Bio-One). Plates containing 100 μL of cell suspension ($5 \times 10^4$ per well) in each well were preincubated for 24 h at 37 °C in a humidified environment with 5% $CO_2$. In the following day, the PA samples were serial diluted in a new 96 well plate. The old media was then replaced by the PA solutions and incubated for 24 h. Samples were run on each plate in triplicate and the final concentrations of PAs ranged from 8 to 256 μg/mL. The plates were further incubated with 50 μL XTT reagent (0.5 mg/mL) at 37 °C for 4 h. The absorbance of the solution was determined at 600 nm using a multiwell plate reader AccuSkan, MultiSkan FC (Thermo Fisher Scientific).

### 2.10. Hemolysis assay

The cytotoxicity against human red blood cells was adapted as described by Nielson et al 2021. Fresh human red blood cells (hRBCs) were washed three times with PBS buffer, centrifuged at 500 × g for 5 min, decanted, and then resuspended in PBS to a concentration of 0.5 ×

$10^8$ cells/mL. PA stock solutions were prepared in ultrapure water at concentrations ranging from 16 to 1024 μg/mL and 25 μL were added to a 384-well plate. Then, 25 uL of cell suspension in PBS was added to each well to a final concentration of $0.25 \times 10^8$ cell/mL. The plate was then shaken for 10 min on a microplate shaker before incubation at 37 °C in 5% $CO_2$ for 60 min, and the cells were pelleted by centrifugation at 1000*g* for 10 min. Lastly, 25 μL of the supernatants were transferred to a new 384-well plate, flat-bottomed plastic 384-well plate and the concentration of hemoglobin was determined by measuring the OD at 405 nm using a BioTek Synergy LX plate reader. The absorbance of the supernatants of cells incubated with 5% Triton X-100 (positive control) were considered 100% hemolysis, ultrapure water was used as a negative control.

### 2.11. pH-dependent cytotoxicity assay

HT-29 cells (ATCC HTB-38) were cultured in McCoy's 5a Medium Modified (ATCC 30–2007) with 10% fetal bovine serum and 1% penicillin/streptomycin. 100 μL of HT-29 cell suspension was added to each well of sterile, polystyrene 96-well plates (Nunclon - Delta Surface treated) at a concentration of 150,000 cells/mL (15,000 cells/well) and incubated at 37 °C in 10% $CO_2$ for 24 h. Following the 24-hour incubation, the culture media was removed and replaced with either 100 μL of fresh media (pH 7.4) or acidified media (pH 6.5). The acidified media was prepared by adding MOPS (3-(N-morpholino)-propanesulfonic acid; Alfa Aesar J62840; CAS 1132-61-2) to reach a concentration of 20 mM, and then lowering the pH to 6.5 using HCl. Stock solutions of the treatment peptides were prepared at 5 mg/mL in deionized water. From the stock solution, treatment concentrations were prepared using 2-fold dilutions with the respective treatment media (pH 7.4 or pH 6.5), ranging from 7.8 μg/mL −500 μg/mL. Water was used as a negative control and Triton-X 100 (Fisher Bioreagents BP151-500; CAS 9002-93-1) was used as a positive control. Cells were incubated at 37 °C in 10% $CO_2$ for 24 h. Following this incubation period, the media was removed from the wells, each well was washed with 100 μL of PBS (phosphate buffered saline; Corning 21-040-CV), and then fresh media (pH 7.4) was added to the wells. The cytotoxicity was measured using an MTT assay kit. 10 μL of 12 mM MTT solution was added to each well, and then cells were incubated at 37 °C in 5% $CO_2$ for 4 h. 100 μL of SDS-HCl was then added and mixed before incubating again at 37 °C in 5% $CO_2$ for 4 h. Wells were then mixed, and absorbance was read at 570 nm using a BioTek Synergy LX plate reader.

### 2.12. In vivo antibacterial studies

*Galleria mellonella* were purchased from Bestbait (Lakeside Marblehead, OH, USA) and maintained on wood chips in the dark. And all assays were followed by the published protocol.[33] Five to nine larvae with a mass of ~160–190 mg each, without darkening of the cuticle, were selected for each step in the procedure. The bacteria suspension was injected into the last left proleg (Hamilton neurons syringe 25 μL, 33-gauge, point style 4, angle 12). The larvae were incubated at 37C for 2–4 days and mortality was recorded daily. **Determination of bacterial infection**: To determine the bacterial infection, 10 μL of various concentrations of *S. aureus* JE2 (MRSA) ($1.5 \times 10^7$ cfu and $1.5 \times 10^8$ cfu) were injected and incubated for 2 days at 37 C to mimic infection in humans. An infective dose of bacteria was determined to cause 60–80% lethality within 48 h, but not 100% lethality within 24 h. ***In vivo* Toxicity testing procedure:** Based on the OECD guidelines, the acute toxicity testing was started by injecting five larvae with the initial dose of a 25 mg/kg. The toxicity testing was continued by retesting at the same dose on new cohort of larvae, if less than 40% lethality was achieved. The experiment continued until a toxic dose was established. ***In vivo* Antibacterial efficacy assay:** First, 10 μL of bacteria at the predetermined infective dose were injected into the last left proleg and incubated for 2 h. After incubating, 10 μL of PA compound or antibiotic was injected to the last right proleg and returned to incubation at 37 ℃. The mortality was recorded daily for 4 days. Vancomycin was used as a positive control. Infected animals without treatment were used as negative control and animals injected with PBS only were also used as a control.

## 3. Results and discussion

### 3.1. Design and characterization of the PAs

According to our previous report[27], the antimicrobial activity and cytotoxicity of PAs are strongly correlated to the length of their hydrocarbon chain. PAs containing an 18-carbon long hydrophobic tail displayed greater antimicrobial activity but also high cytotoxicity against human cells (including HEK-293 and red blood cells) than the counterparts with shorter alkyl tails. The 16-carbon length PAs showed a diminished antibacterial activity but lower toxicity against human cells compared to their 18-carbon counterparts. Aiming to develop more selective PAs and further study the effects of the 16-carbon length hydrophobic tail in the antibacterial activity of these peptides, we designed cationic PAs with a 16-carbon hydrophobic tail while varying their amino acid sequence. In particular, we studied Lysine (Lys), Arginine (Arg), Histidine (His), and Tryptophan (Trp). Lys, Arg are known as important cationic amino acids that interact with negatively charged lipids present in bacteria membranes[34] while the replacement of Lys with His residues have shown decreased cytotoxicity while maintaining antibacterial activity.[35] Trp residues are known to facilitate bacteria membrane disruption and improve the activity of antimicrobial peptides due to its hydrophobic characteristics. Trp interacts with the interface region in the membrane, helping the peptide to anchor to the bilayer surface.[36] We also designed PAs containing a 18-carbon length tail to diaminopropionic acid (Dap). Dap is a non-proteinogenic amino acid, with shorter side chain (1 methylene unit, less hydrophobic) than Lys. This amino acid has a $pK_a \sim 6.0$ which will be deprotonated at physiological pH. However, there is most likely a small variation since the $pK_a$ values for amino acids can vary depending on the chemical environment and proximity to the core of the nanostructure, similar to the shifts of pKa that happens in folded proteins.[37,38] The structure of the designed PAs, the morphology of the self-assembled structures they form, and their physical chemical properties are summarized in Table 1.

The chemical structures, mass spectra and purity of the compounds can be found in the Supporting Information (SI1). The morphology of the self-assembled nanostructures was assessed by transmission electron microscopy (TEM) and shown in Fig. 1 and Fig.SI5. As expected, PA1, PA2, PA3, and PA6, PA7, PA8 and PA9 self-assembled into micelles, a morphology driven by the hydrophobic collapse of the tails and the repulsion between the charged residues.[39] PA2 formed micelles with 7 +/−1 nm width. The size of the other nanostructures could not be determined because they were too small for accurate measurement with our instruments.. Interestingly, we expected that PA3 would self-assemble into fibers due to Ala residues adjacent to the hydrophobic tail that have propensity to for β -sheets. A possible factor that leads to the formation of micelles instead of nanofibers could be related with the ionic strength and strength of the intramolecular bonding[39] since both hydrophobic interactions and hydrogen bonding are present in the same molecule, the decreased ionic strength increase the electrostatic repulsion of the charged residues[40] favoring the formation of micelles. PA3 only contains 3 Ala residues, which is not enough to produce sufficient H-bonds to offset the electrostatic repulsion. According to previous report, the formation of fibers is favored by 4 amino acid residues forming β-sheet hydrogen bonds close to the core.[41] This could also be observed in PA7, which contain 2 Ala residues and self-assemble into micelles (Table 1). PA4 did not self-assemble into nanostructures possibly due to the bulky Trp residues being placed at the C-terminus of the peptide structure. The lack of backbone H-bonding and the electrostatic repulsions near the hydrophobic portion could be other factors

**Table 1**
Sequence, morphology, and physicochemical properties of PAs.

| PAs | Sequence[a] | Morphology by TEM | Charge at pH 7[b] | Charge at pH 5.5[b] | Zeta Potential (mV)[c] | Retention Time (min)[d] |
|---|---|---|---|---|---|---|
| PA1 | $C_{16}$KHKHK | Spherical micelles | +3 | +5 | 15.8 ± 1.9 | 13.4 |
| PA2 | $C_{16}$KRKR | Spherical micelles | +4 | +4 | 15.0 ± 8.8 | 13.8 |
| PA3 | $C_{16}$AAAKRKR | Spherical micelles | +4 | +4 | 10.8 ± 6.4 | 14.3 |
| PA4 | $C_{16}$KKKWW | Amorphous | +3 | +3 | 47.0 ± 2.0 | 15.2 |
| PA5 | $C_{16}$FFFKKKK | Nanofibers | +4 | +4 | 11.9 ± 3.9 | 16.2 |
| PA6 | $C_{18}Dap_5$ | Spherical micelles | 0 | +5 | 13.7 ± 2.4 | 14.6 |
| PA7 | $C_{18}AADap_3$ | Spherical micelles | 0 | +3 | 10.3 ± 3.2 | 15.9 |
| PA8 | $C_{18}HHDap_3$ | Spherical micelles | 0 | +5 | 30.4 ± 3.6 | 14.4 |
| PA9 | $C_{18}RRDap_3$ | Spherical micelles | +2 | +5 | 30.1 ± 4.4 | 14.6 |

[a] Lysine (K, Lys), arginine (R, Arg), phenylalanine (F, Phe), alanine (A, Ala), histidine (H, His), tryptophan (W, Trp), Dap (DAP (2,3-diaminopropionic acid), hexadecanoic acid (C16) and octadecanoic acid (C18).
[b] Estimated charges based on $pK_a$ values for individual amino acids.
[c] Aqueous solution of 250 μg/mL concentration at pH 7.
[d] Retention time obtained from RP-HPLC analysis using a linear gradient method of ACN:$H_20$ containing 0.1% TFA (0–100% 20 mins).

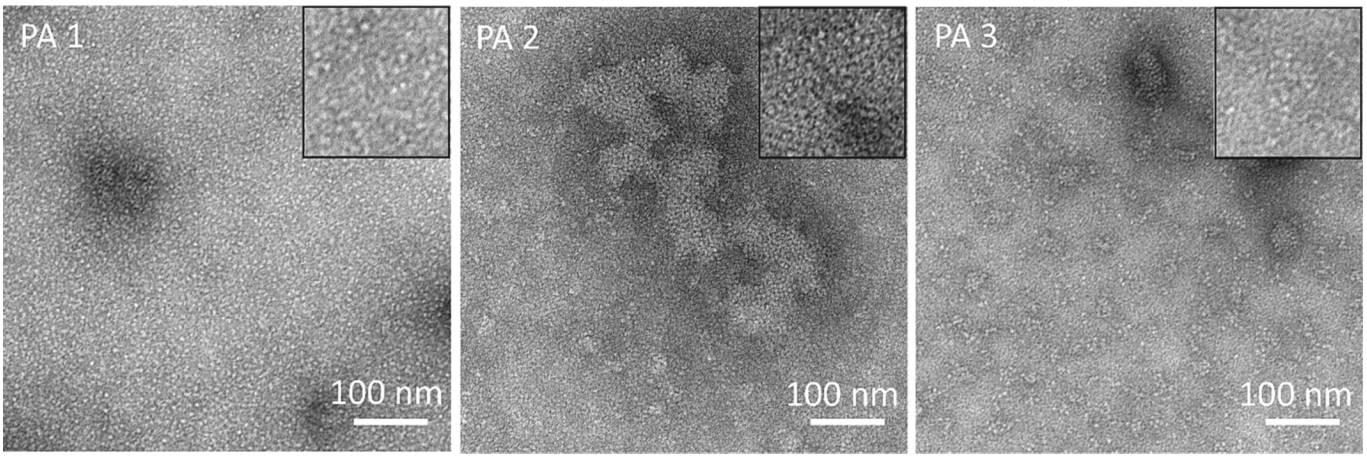


**Fig. 1.** Morphology of PA 1, PA 2, and PA 3 assemblies observed by TEM. PA was prepared at 1 mg/mL in HPLC grade water, annealed, and aged overnight before imaging. Scale bar 100 nm. All these three PAs formed 6–7 nm diameter spherical micelles.

influencing the formation of well-defined nanostructures. PA5 self-assembled into nanofibers with ~9 nm of diameter, due to the π-π stacking of the phenylalanine residues, which also works as a promoter for both α-helix and β-sheet. Thus, a better ability for fibril formation is achieved when compared to PA5. TEM images for selected PAs are shown in Fig. 1, while the rest of the other TEM images can be found in the Supporting information (SI 5).

Charge and hydrophobicity have been described to be important for antimicrobial activity of peptides. The positive charge facilitates the interaction with the slightly negative bacteria membrane and the hydrophobic alkyl chain permeates it, potentially leading to membrane damage. We studied the zeta potential to determine surface charge and hydrophobicity of the PAs and the values are shown in Table 1. All peptides showed positive zeta potential values ranging from +10.3 to +47 mV. PA3, PA5, PA6 and PA7 are considered nearly neutral with zeta potential values around +10 mV. PA6 and PA7 are composed by Dap as a cationic residue which is not expected to be protonated at pH 7, which is consistent with the lower zeta potential values. The relatively smaller zeta potential values of PA2, PA3, and PA5 indicate a weaker electrostatic repulsion between individual PA molecules that can be related to their morphology. PA2 and PA3 self-assembled into small spherical micelles and some aggregation can be observed from TEM, indicating the tendency for particles to come together. Meanwhile, the entangled PA5-fibers suggest fiber–fiber attraction, probably due to the compromise repulsion due to intermolecular π-π interactions and H-bondings.[42] High repulsive forces between adjacent PA fibers could discourage any lateral assembly/entangle/aggregation.[43] PA4, PA8 and PA9 had large positive zeta potential values being considered strongly cationic. The zeta potential results for PA4 could be explained by the fact this peptide is not self-assemble into nanostructures having all the positive charged residues exposed to the solvent. We also determine the relative hydrophobicity of the PAs using RP-HPLC, retention times are listed in Table 1. As expected, PAs with a C18 alkyl chain were among the most hydrophobic PAs showing higher retention time in between 14.44 and 16.19 min. PA4 and PA5 have a C16 alkyl chain but displayed a higher hydrophobicity due to the presence of Phe and Trp residues.

### *3.2. PAs shown potent broad-spectrum antibacterial activity against all the strains tested*

The antibacterial activity of the PAs against gram-negative and gram-positive strains was determined using the broth microdilution method. MIC values are summarized in Table 2. PA2 and PA3 displayed potent antibacterial against all tested strains with a geometric mean of MIC values of 6 μg/mL and 7 μg/mL respectively (MICs ranging from 4 to 8 μg/mL). These PAs are formed by cationic amino acids, Lys and Arg residues are known to have an important role in the activity of Antimicrobial Peptides (AMPs), and they can form hydrogen bonds, electrostatic interactions, and cation-$\pi$ interaction facilitating the interaction with negatively charged lipids such as lipopolysaccharides and phospholipids in the bacteria membrane[34].

The order of increased zeta potential is as follows: PA7 < **PA3** < PA5 < PA6 < **PA2** < PA1 < PA9 < PA8 < PA4 (Table 1). The most active peptides, PA2 and PA3 (in bold) have small zeta Potential values of 15.0 mV and 10.0 mV, respectively (Table 1). PA1 has a slightly greater Zeta Potential compared to PA2 and also a lower antibacterial activity,

**Table 2**
Minimum Inhibitory Concentration (MIC) of PAs against selected bacteria strains.

| PAs | Sequence | MIC (μg/mL) | | | | | |
|---|---|---|---|---|---|---|---|
| | | *Ec*[a] | *Ab*[b] | Sa[c] | Sa[d] | Sa[e] | G.M. |
| PA1 | $C_{16}$KHKHK | 32 | 64 | 64 | 32 | n.e. | 45. |
| PA2 | $C_{16}$KRKR | 4 | 8 | 4 | 8 | 8 | 6. |
| PA3 | $C_{16}$AAAKRKR | 8 | 4 | 8 | 8 | 8 | 7. |
| PA4 | $C_{16}$KKKWW | 128 | 64 | 128 | 32 | n.e. | 76. |
| PA5 | $C_{16}$FFFKKKK | 64 | 64 | 64 | 64 | n.e. | 64. |
| PA6 | $C_{18}Dap_5$ | 32 | 64 | 32 | 16 | n.e. | 32. |
| PA7 | $C_{18}AADap_3$ | 32 | 64 | 32 | 64 | n.e. | 45. |
| PA8 | $C_{18}HHDap_3$ | 64 | 64 | 64 | 32 | n.e. | 54. |
| PA9 | $C_{18}RRDap_3$ | 32 | 32 | 32 | 16 | n.e. | 27. |
| Vancomycin | | n.e. | n.e. | 0.5 | 1 | 2 | |
| Gentamicin | | 1 | 1 | n.e. | n.e. | n.e. | |

n.e. = not evaluated [a]*Escherichia coli* K12, [b]*Acinetobacter baumannii* (patient isolated from Nebraska Medicine), [c]*Staphylococcus aureus* JE2 MRSA, [d]*Staphylococcus aureus* 13C MRSA, [e]*Staphylococcus aureus* LAC MRSA. G.M. = geometric mean.

suggesting that there is a smaller range of values that correspond to biological activity. Another important characteristic of these active peptides is their self-assembling morphology. PA2 and PA3 self-assembled into micelles, and these results support our previous findings that the antibacterial activity is also dependent of the morphology of the nanostructures with micelles demonstrating more potent antibacterial activity compared to nanofibers.[27] Our proposed mechanism of action is that micelles disassemble in contact with bacteria membrane and the hydrophobic moiety of single molecules interact with bacteria membrane and penetrating the lipid bilayer leading to membrane damage. Thus the stability of the nanostructure also plays an important role since micelles in general are less stable compared to nanofibers.[27] The zeta potential experiments are an important tool to determine not only the nanostructure surface charge and propensity to form aggregates but also the stability of the nanoparticles.[44] The smaller zeta potential (generally smaller than +/−30 mV) values of these peptides indicate low physical stability of the nanostructures which can be related with their potent antimicrobial activity. A recent study investigated the relationship between physical properties and antimicrobial activity of PAs, their findings indicate that less stable nanofibers disassemble in solution resulting in higher antibacterial activity in contrast to more stable nanofibers, which can attach to the bacteria membrane but do not have the ability permeate the membrane leading to lower antibacterial activity. [45] Together, these findings further support our proposed mechanism of action of PA micelles.

The order of increasing relative hydrophobicity of the designed PAs determined by RP-HPLC is as follows: **PA1** < **PA2** < **PA3** < PA8 < PA9 < PA6 < PA4 < PA7 < PA5 (Table 1). The most active PAs, PA2 and PA3, were among the less hydrophobic PAs with retention times of 13.8 and 14.3 min, respectively. This data also suggests that there is a hydrophobicity range ideal for antibacterial activity. It is worth mentioning that PA5 and PA6 are within the zeta potential range for antibacterial activity between ~ 10–15 mV, but they were more hydrophobic than PA2 and PA3, thus falling outside of the hydrophobicity range (~13–14 min) for the antimicrobial activity. This high hydrophobicity might be linked to their lower antibacterial activity.

The PAs containing His and Dap in their sequence, PA1 and PA6-PA9, demonstrated moderate to lower antibacterial activity with higher MIC values ranging from 16 to 128 μg/ml. His ($pK_a$ ~ 6.3[46]–6.5[47] and Dap ($pK_a$ ~ 6.3[48]) has a neutral side chain at pH 7 with overall charge of these peptides ranging range from 0 to +3, which could explain their lower antibacterial activity. The antimicrobial activity of His rich peptides is reported to be enhanced by acidic pH environments.[47,49] The pH sensitive peptides can be extremely beneficial clinically because it potentially restricts the antibacterial activity to certain compartments of the cellular environment (i.e., acidified phagosome) or certain tissues and organs. This approach can potentially increase selectivity of the peptides since the excessive net charge is reported to cause cytotoxicity,[50] Leveraging pH sensitive peptides is a great opportunity to develop future pH-dependent drug delivery systems with synergistic mechanism of action. Moreover, the replacement of Lys and Arg with Dap in the polar face of AMPs is reported to eliminate lysis of human red blood cells while maintaining the antibacterial activity.[51] We evaluated the antimicrobial activity of PA1, PA2, PA7-PA10 at pH 5.5 against *S. aureus JE2* and *E.coli* K12, however the difference in MIC values were generally small- either equal or 1 fold-increase in activity compared to the MIC at pH 7.0 (Supporting Information SI6), and these small differences likely have minimal physiological relevance. We were expecting a better antimicrobial activity, especially for PA7 and PA9, which are completely neutral at pH 7 and have a +5 charge at pH 5.5. However, we now believe that the short side chain of Dap (1-carbon length) is less available to bind and interact with negative charge lipids in the membrane, thus not leading to an increased antibacterial activity. This is also known as "snorkel effect", which explains that longer aliphatic side chain (i.e. lysine and arginine) of the positive charged residues are able to insert deeply into the lipid membrane while still interacting with negatively charged lipid membrane on the surface.[52,53] Together, our findings and data in the relevant literature explain the relatively poor antibacterial activity of PA7, PA8, PA9 and PA10.

Tryptophan has been reported to enhance antibacterial activity of peptides due to its hydrophobic and bulky side chain that facilitates the binding of the peptide to the lipid bilayer via interactions with the interfacial area of the cell membrane, therefore we would expect that PA5 would present antibacterial activity.[54] The positively charged Lys residues in the PA5 are (most likely) less available to interact with LPS in the bacterial membrane because they are placed between the long hydrocarbon chain and two bulky tryptophan residues, making it more difficult to target the membrane via electrostatic interactions. In addition, PA5 does not self-assemble into a well-defined nanostructure. Together, our findings suggest that the antibacterial activity is not only related to the proper balance of charge and hydrophobicity, the amino acid composition, the morphology of self-assemble and the stability of these nanostructures most likely also play an important role in their interaction with bacterial membrane.

Lastly, we tested the ability of PA2 to inhibit the formation of biofilms and disrupt biofilm. PA2 was not able to disrupt pre-formed S. aureus JE 2 biofilms at the MIC, 2 times MIC and 4 times MIC concentrations, however PA2 was able to inhibit the formation S. aureus JE 2 biofilm at MIC concentration (Methods and results are described in the Supporting Information SI7).

### 3.3. PA1 potentiates the activity of vancomycin against E. coli leading to a synergistic antibacterial activity

We tested some selected PAs based on their antibacterial activity, in combination with Rifampicin and Vancomycin to evaluate synergistic antibacterial activity using a checkerboard assay. Drug combinations with FICi below 0.5 indicates a synergistic antibacterial effect and FICi between 0.5 and 4 indicates an additive or indifferent effect[11]. To be considered a good antibiotic adjuvant candidate, it should exhibit a synergistic effect with antibiotics with FICi below 0.5 associated with a low antibacterial activity (higher MIC value) of the antibiotic alone.

Rifampicin is a lipophilic antibiotic that inhibits the synthesis of RNA by binding the DNA-dependent RNA polymerase,[55] and it is not typically used against gram-negative bacteria due to limitations in the membrane permeability. Fig. 2 shows the checkerboards of PA2 and PA3 in combination with Rifampicin against *E. coli* and *A. baumannii*. PA2 and PA3 alone displayed antimicrobial activity against *E. coli* and *A. baumannii,* as described previously, with MICs ranging from 4 to 8 μg/mL (Table 2). Thus, if rifampicin shows increased antibiotic activity against gram-negative bacteria in combination with PAs, then it would likely suggest synergistic or additive activity due to PA-induced membrane

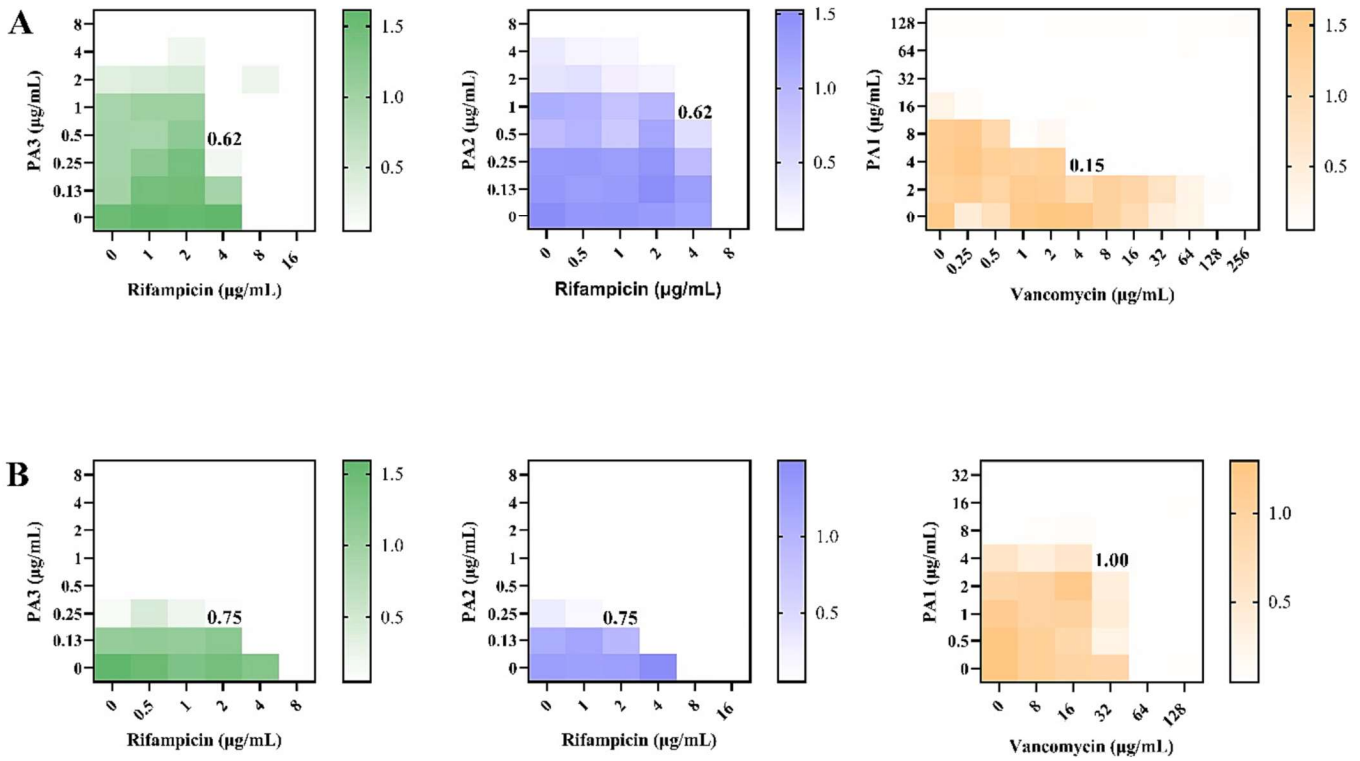


**Fig. 2.** Synergistic screening of selected PAs in combination with antibiotics. A) Checkerboards of PA3 (left) and PA2 (middle) in combination with Rifampicin and PA1 (right) in combination with Vancomycin against *E. coli.* B) Checkerboards of PA3 (left) and PA2 (middle) in combination with Rifampicin and PA1 (right) in combination with Vancomycin against *A. baumannii.* FICi's are shown in the figure. Selected antibiotics were tested at 2-fold serial dilutions across the plate in combination with 2-fold serial dilutions of the selected PAs down the plate, where the last column and the last row in the plate contain two-fold dilutions of antibiotics and peptides alone to determine their MIC.

permeability. Rifampicin (MIC = 8 μg/mL against *A. baumannii* and *E. coli*) presented a 2-fold increase in antibacterial activity against *A. baumannii* in combination with PA2 and PA3 with FICi of 0.75, whereas rifampicin displayed an 8-fold increase in antibacterial activity against *E. coli* when in combination with PA3 and PA4 with FIC of 0.67, indicating an additive effect or "no interaction" between these drugs.[56] In general, the outer membrane permeabilizer compounds that potentiate the activity of gram-positive antibiotics in gram-negative strains present very low or no antibacterial activity alone,[57] a well-known example is the Polymyxin B nonapeptide (PMBN) which possess a very low antibacterial activity alone but is able to potentiate the antibacterial activity of several antibiotics against gram-negative bacteria including Rifampicin.[58] Thus, the "no interaction" between PA2 and PA3 with rifampicin could be explained by the fact that these PAs already present antibacterial activity alone.

Gram-negative bacteria are intrinsically resistant to vancomycin blocking its access to lipid II target.[9] We evaluated the effect of PA1, a compound with low antibacterial activity (MIC = 32 μg/mL against *E. coli*) in combination with vancomycin against *E. coli* (Fig. 2). The findings of this combination were very interesting as vancomycin exhibited a 32-fold increase in antibacterial activity with the presence of PA1 ($MIC_{Vanco}$ = 128 μg/mL and $MIC_{Vanco+PA1}$ = 4 μg/mL). Thus, PA1 can work as a membrane-targeting compound to potentiate the activity of vancomycin. In addition, the activity of PA1 itself is also enhanced by the presence of vancomycin asPA1 exhibits an 8-fold increase in antibacterial activity ($MIC_{PA1}$ = 32 μg/mL and $MIC_{PA1+Vanco}$ = 4 μg/mL), leading to a synergistic antibacterial activity with FICi of 0.15.

In addition, we tested the PA1 and PA5 in combination with vancomycin against *A.baumannii*. We observed no significant effect of these combinations which can be explained by the more permeable OM of *E. coli* compared to *A. baumannii.* A. baumanni produces a hepta-acylated lipid A compared to the hexa-acylated lipid A of E. coli, which increases the hydrophobicity in the membrane. In addition, it can survive in absence of lipooligosaccharide and Lipid A, the latest known to be essential for cell survival[59].

Vancomycin is a large hydrophilic molecule, which is usually not effectively sensitized by cationic agents that increase the outer membrane permeability like pentamidine, for example. These agents alter the LPS outer leaflet facilitating the diffusion of drugs across the outer membrane, but they do not damage the integrity of the outer membrane causing membrane disruption. These changes are not enough to facilitate the uptake of large hydrophilic molecules like Vancomycin.[60,11,61] Unlike PAs, cationic agents such as pentamidine do not present an hydrophobic moiety on their structures affecting the ability of these molecules to deeply permeate the lipid membrane. The "derivatization-for-sensitization approach" is described in the literature as a successful strategy to sensitize vancomycin and increase drug uptake.[61] In this approach, a combination of a vancomycin-derivative containing a lipocationic moiety and a symmetric di-cationic small molecule leads to membrane disruption by cooperative membrane binding and promotes the uptake of vancomycin. It is worth mentioning that only a few of vancomycin's drug adjuvants described in the literature present cationic and hydrophobic characteristics.[61] Those molecules are similar to our PAs (cationic and hydrophobic), which may work as new molecules with the ability to sensitize gram-negative pathogens against vancomycin. Together, these findings indicate that the ability of the PAs to sensitize antibiotic drugs is probably strongly related to their ability to change membrane permeability.

### 3.4. PAs affect the inner-membrane permeability of E. coli

To have some insights on the mechanism of action of PA1 + vancomycin drug combination, PA2, and PA3, we studied inner membrane (IM) permeability using a Propidium Iodide uptake assay. The

fluorescence intensity of PI in cells treated with PAs and the drug combination are shown in Fig. 3A. Polymyxin B was used as a positive control to indicate increased inner-membrane permeability. The results show that PA1 at 4 μg/mL (1/8 of the MIC) presents a relatively smaller PI fluorescence compared to other treatments indicating low permeability of the IM, however the cells treated with PA1 at 1 × MIC (32 μg/mL) and 2 × MIC (64 μg/mL) have shown considerably higher PI fluorescence when compared to the positive control polymyxin B indicating greater IM permeability. The drug combination (PA1 + vancomycin) at concentrations of 4 μg/mL:4μg/mL (FICi) showed an increased PI fluorescence compared to the untreated control and the combination at 2 × FICi exhibit greater PI fluorescence compared to the positive control polymyxin B. As expected, vancomycin alone did not induce membrane permeability at 4 μg/mL (1/32 of the MIC) and at the MIC value of this drug alone (MIC = 128 μg/mL). Together these results indicate that PA1 alone increases the IM permeability in a dose-dependent manner, and PA1 in combination with vancomycin presents a synergistic mechanism of action that further increases the inner-membrane permeability of *E. coli* in consequence of bacteria death, since these drugs alone did not induce IM permeability at the FICi concentrations.

Since the PA molecules present both cationic and hydrophobic characteristics, we proposed that 1) PA1 is able to disrupt the inner membrane of *E. coli* in a dose-dependent manner causing a small permeabilization at sub-MIC concentrations. Also, we hypothesize that at sub-MIC concentrations PA1 is able to fully disrupt the outer membrane of the *E. coli* with little effect on the inner membrane. 2) The cationic moiety of the PA1 targets the negatively charged lipids in the outer membrane and the lipid tail then permeates the hydrophobic bilayer causing outer membrane damage/ disruption and increasing permeability. 3) As a result, there is a rapid increase in the accumulation of vancomycin in the cells and in combination with the metabolic perturbations lead to greater cell death. 4) Vancomycin is known to bind to the d-Ala-d-Ala terminus of the peptidoglycan (PG) cell wall precursor lipid II and prevent synthesis of cell wall.[62,63] 5) PA1 and Vancomycin behave

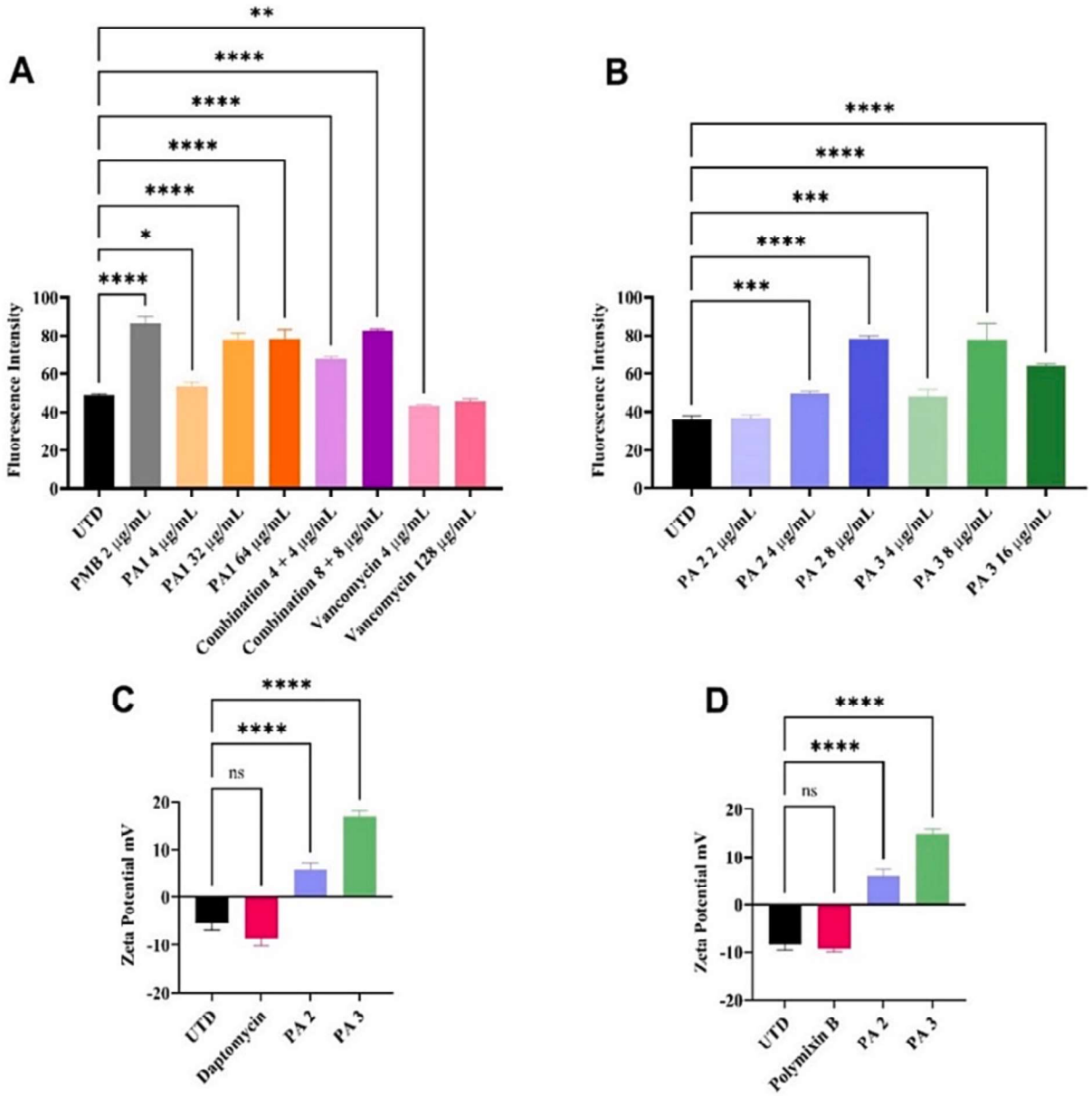


**Fig. 3.** Mechanism of action of PAs on bacteria membrane. A) Propidium iodide uptake of *E. coli* K12 treat with PA1 and PA1 in combination with Vancomycin at different concentrations. B) Propidium iodide uptake of *E. coli* K12 treat with PA2 and PA3. C) Zeta Potential of *S. aureus* MRSA JE2 after treatment with PA2 and PA3 at 40 μg/mL and 80 μg/mL, respectively. D) Zeta Potential of *E. coli* K12 after treatment with at 40 μg/mL and 80 μg/mL, respectively. *Represents p less than 0.05.

differently when used alone but when used in combination these drugs displayed increased inner membrane permeability. These findings suggest a cooperative mechanism of PA1 and Vancomycin that increases the inner membrane permeability of these drugs in combination. Fig. 4 illustrates the proposed mechanism of action of these drugs in combination. A similar mechanism is also proposed for antimicrobial hexadecapeptide used in combination with vancomycin[64].

Fig. 3B shows the PI uptake assay of *E. coli* cells treated with PA2 and PA3 at different concentrations. The PA2 at 4 μg/mL (1/2 MIC) did not show significant PI fluorescence, PA2 at 8 μg/mL (MIC) and 16 μg/mL (2 × MIC) presented an increased PI florescence indicating inner membrane permeability. Similar results were observed when *E. coli* was treated with PA3. Both PA2 and PA3 indicate inner membrane permeability in a dose-dependent manner.

The Zeta potential studies have been reported as an important tool to study the interaction of cationic compounds with bacteria membranes surface because these interactions are mostly governed by electrostatic interactions between the positively charge PAs and negatively charged bacteria membrane in addition to hydrophobic interactions.[65,66] We studied the changes in the bacteria membrane potential of MRSA E. coli after treatment with PA2 and PA3 and the results are presented in Fig. 3C and 3D. Daptomycin and Polymyxin B were used as standard drugs for MRSA and *E. coli* respectively.

Zeta potential of untreated MRSA and E coli were found to be –5.52 mV for MRSA and −8.44 mV for *E. coli*. The higher negative electric potential of untreated *E.coli* cells compared to MRSA is attributed to the additional layer of negatively charged LPS present in gram-negative bacteria, these results are similar to other reports in the literature.[65,67] Daptomycin and Polymyxin B did not significantly change the membrane potential of MRSA and *E.coli* at 20 μg/mL, which is correspondent to 10 × MIC for the drugs. These can be explained by the lower concentrations used in our assays. According to the previous report, Polymyxin B failed to change the membrane potential of MRSA and the changes observed in *E. coli* were dose dependent showing about 10% of zeta potential change at lower concentrations as used in our assay.[65] Daptomycin has an anionic characteristic, it binds to $CA^{2+}$ ions in present in the membrane, which gives it amphiphilic character similar to AMPs[68], these mechanism could explain why Daptomycin does not cause changes in the membrane potential.

However, PA2 and PA3 have shown a significant shift in the zeta potential with positive values for both MRSA (Fig. 3C) and *E.coli* (Fig. 3D) after 1 h treatment at 40 μg/mL of PA2 and 80 μg/mL of PA3 (10 × MIC) compared to the untreated control. These findings show that PA2 and PA3 neutralized the membrane surface charge, destabilizing the membrane and increasing the permeability. The surface charge neutralization has been directly linked to increased membrane permeability in previous studies.[69] These findings are supported by the PI uptake assays showing increase of membrane permeability of E. coli cells at even lower concentrations of 1 × MIC.

We further investigated the effect of PAs on bacteria cells morphology by SEM (Fig. 5). *S. aureus* and *E. coli* showed substantial morphology changes on membrane surface presenting severe membrane deformations with protruding bumps, holes, and cytoplasmatic leakage after treatment with PA2. Untreated *S. aureus* and *E. coli* showed a smooth and normal membrane surface as seen in Fig. 5. Together these results indicate that the mechanism of action of PAs is associated with membrane damage, which is supported by other reports in the literature.[27,70]

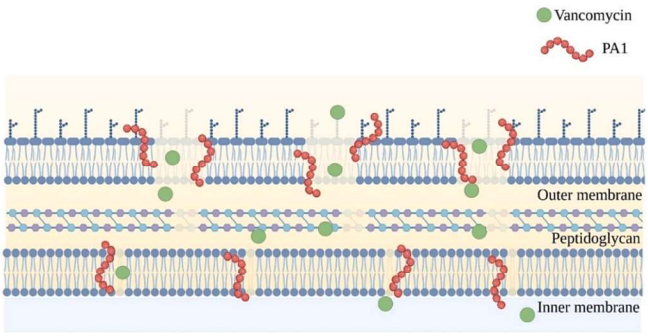


**Fig. 4.** Proposed mechanism for synergistic antibacterial activity of the drug combination (PA1 + Vancomycin) in *E. coli*.

### 3.5. PAs show a low rate of resistance over a period of 21 days

We studied the resistance generation rate for selective PAs against MRSA JE2 (Fig. 6A) and *E. coli* K12 (Fig. 6B) using the microdilution in broth method over a period of 21 days. As shown in Fig. 6A, the MIC of PA2 against *S. aureus* did not change over 21 days indicating that PA2 was not susceptible to drug resistance while PA3 exhibit a two-fold increase of MIC after day 5. Vancomycin also exhibits a two-fold increase of MIC after 19 days. The low rate of resistance for PA3 and the lack of resistance displayed by PA2 is likely due to their mechanism of action associated with membrane disruption. In contrast PA1 alone and PA1 in combination with vancomycin displayed an 8-fold increase of MIC over a period of 21 days with slower development of resistance for PA1 alone. Gentamycin did not show significant susceptibility to drug resistance during the tested period. We believe that PA1 alters the membrane permeability but does not disrupt the membrane facilitating the development of resistance over time. The mechanism of resistance in PA1 could be mediated by changes in the membrane surface by increasing the positive charge, which leads to electrostatic repulsion, similar to the mechanism of daptomycin resistance.[71]

### 3.6. Cytotoxicity

We evaluated the toxicity of selected PAs against HEK-293 using the XTT assay and the cell viability is shown in Fig. 7A. PA2 and PA3 did not present toxicity against the cell line tested up to 8–16 × MIC values. PA1 also did not present toxicity to the cells up to 16 × MIC of PA1, compared to the concentration of antimicrobial activity in combination with vancomycin (MIC = 4 μg/mL). Overall, the cells exhibit about 100% of viability up to a concentration of 64 μg/mL, which is much lower compared to their MIC values against all bacteria strains tested. These results show the great potential of the PAs as antibacterial drugs encouraging us to further study the mechanism of action and the efficacy of these PAs in *in vivo* models in the future.

We also studied the hemolytic activity (Supporting Information SI8) of the PAs against red blood cells and the % of hemolyzed cells at 8 μg/mL are shown in the Fig. 5B. PA1 shows 28.2 % of cell lysis at 8 μg/mL, and this concentration corresponds to 2 × *FICi* of the PA1 in combination with Vancomycin. We expect that PA1 will have a lower hemolytic activity at the *FICi* concentration, but still more studies are needed in order to develop more selective PAs. PA3 and PA4 show 33.3% and 30.6 % of cell lysis at 8 μg/mL, respectively. We observed some correlations between the hemolytic activity, hydrophobicity, and charge among the designed PAs. The most hemolytic PA9 at the concentration tested showed lower zeta potential values and higher hydrophobicity compared to the less hemolytic PA8. Both PA 2 and PA3 (the best antibacterial PAs) were less hydrophobic than PA8, which is shifted toward less hydrophobicity, however both PA2 and PA3 presented a lower positive zeta potential compared to PA8. Hemolytic activity has been linked to higher hydrophobicity which is an important characteristic of membrane active peptides. More studies of structure–toxicity relationship and the development of new strategies such the use of D-amino acids for example are necessary to improve the therapeutical window of these PAs.[72] In addition, the use and development of other potential drug combination therapies with synergistic mechanism of action similar to what we found with PA1 and Vancomycin may lead to new approaches that requires lower concentrations of drugs to achieve

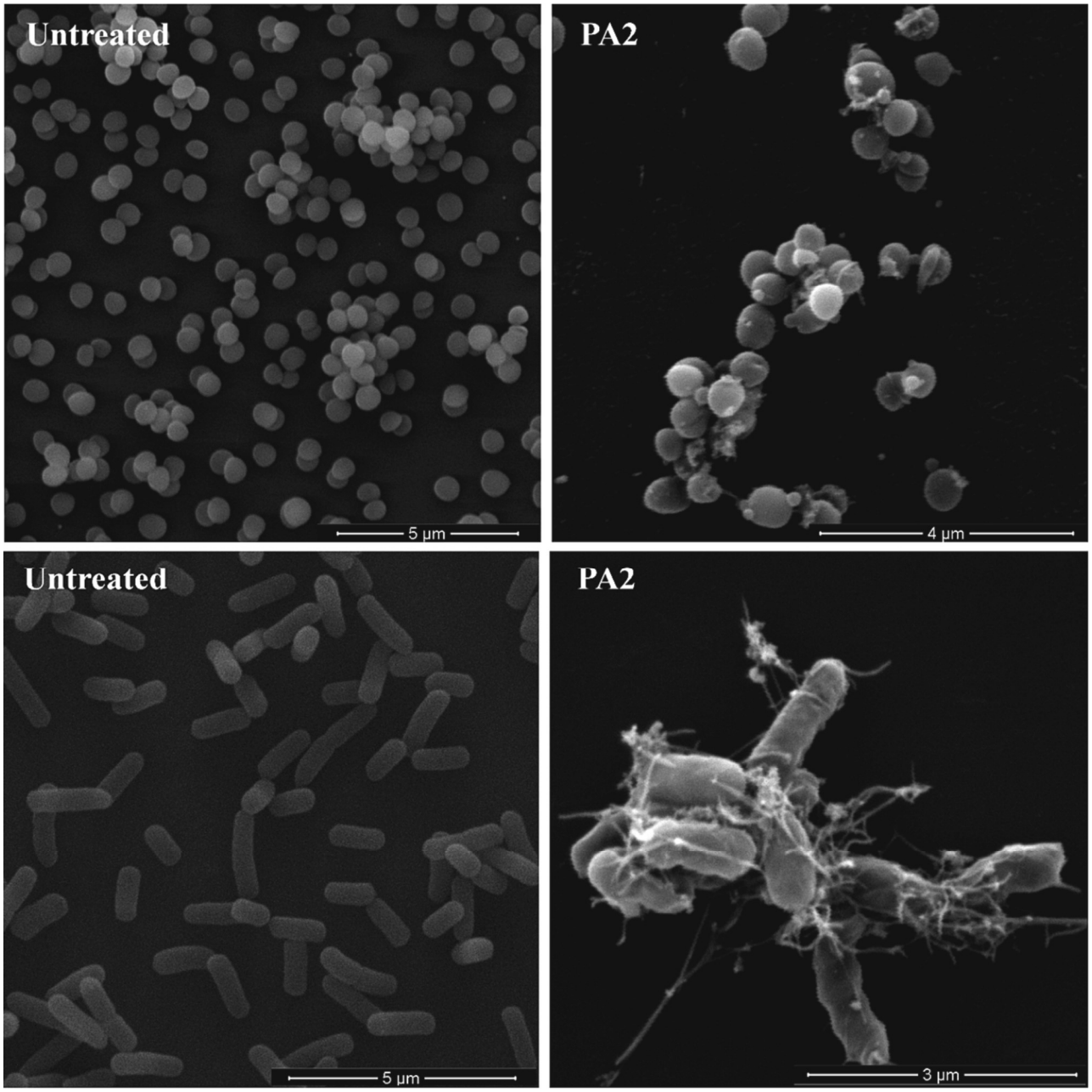


**Fig. 5.** SEM micrographs of *S. aureus* (top) and *E. coli* (bottom) after treatment with PA2 at 8 μg/mL (2X MIC). Untreated bacteria (with no PA addition) were used as a control.

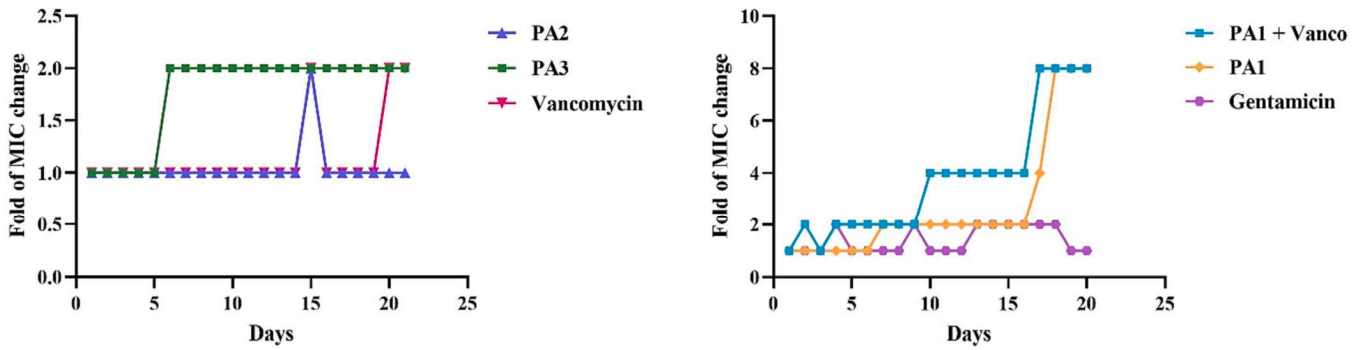


**Fig. 6.** Resistance generation studies. A) Resistance generation for PA2, PA3 and Vancomycin against *S. aureus* MRSA JE2 over 21 days. B) Resistance generation studies for PA1, PA1 in combination with Vancomycin (1:1 ratio) and Gentamicin against *E. coli* K12 over 21 days.

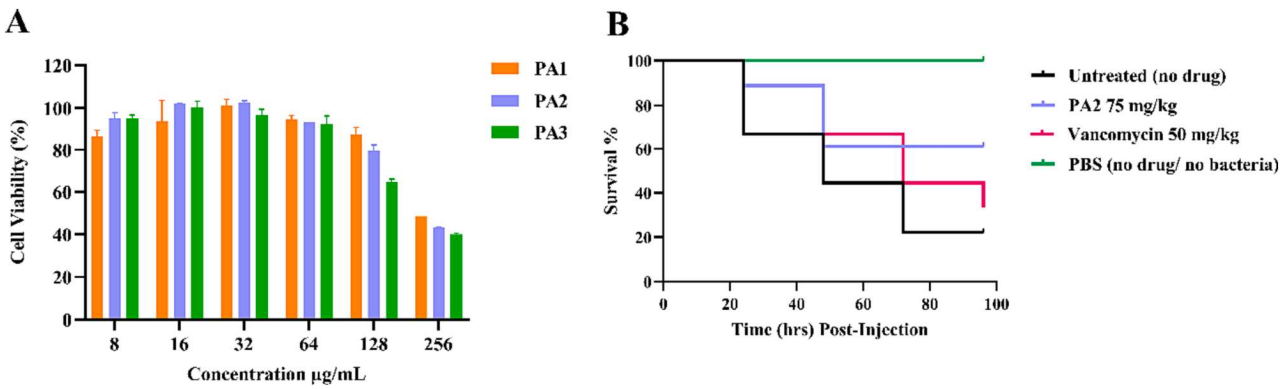


**Fig. 7.** Toxicity of selected PAs. A) Cytotoxicity of selected PAs against HEK-293 cells using XTT assay. B) Antibacterial *in vivo* assay against MRSA JE2 infection in *G. mellonella* model.

antibacterial activity. The use of lower concentrations as an approach is another strategy to overcome the potential toxicity of these PAs."

Due to the pH response activity of the Dap rich peptides and the similarities in charge of bacteria cell membrane and cancer cells, the viability of HT-29 cells following treatment with PA6, PA7, PA8 and PA9 was determined in both physiological (pH 7.4) and acidic (pH 6.5) conditions using the MTT assay. The cancer cell membranes are negatively charged with extracellular pH of 6.2–6.9 which is similar to the negatively surface charge of bacteria membrane, this characteristics of cancer cell membranes is due to the presence of negatively charged lipids such as phosphatidylserine and phosphatidylethanolamine in the outer leaflet compared to normal cell membrane where these lipids are present in the inner leaflet.[73] Increases in the $IC_{50}$ values for the physiological conditions compared to the acidic conditions were observed for every PA with an $IC_{50}$ that was measurable within the tested concentrations. PA 6 had $IC_{50}$ values of 61.8 µg/mL at pH 6.5 and 71.7 µg/mL at pH 7.4. PA 8 had $IC_{50}$ values of 72.3 µg/mL at pH 6.5 and 126.4 µg/mL at pH 7.4. PA 9 had $IC_{50}$ values of 81.7 µg/mL at pH 6.5 and 117.3 µg/mL at pH 7.4. These results indicate a decrease in cytotoxicity in physiological conditions (pH = 7.5) for PA6, PA8, and PA9. PA 7 showed no measurable $IC_{50}$ value at both pH conditions, indicating low cytotoxicity at the tested concentrations. Cells in acidic conditions treated with 125 µg/mL of PA8 neared complete loss of viability, and at 250 µg/mL, no viable cells remained. However, when cells in physiological conditions were treated with PA8, viable cells remained even at the highest treatment concentration, 500 µg/mL (Supporting Information, Fig. SI9), suggesting that the cytotoxicity might be related to charged residues. Even though these peptides presented a relatively higher hydrophobicity, the lower toxicity of these peptides at pH 7 could be attributed to the amino groups of the side chain being nearly deprotonated and neutral. The PA6, PA7 and PA8 present a net charge of 0 at pH 7 and PA10 present a +2 charge at pH7. The positively charged residues in PA6 are near to the side chain and not at the surface of the micelle, possibly explaining the lower toxicity.

### *3.7. In vivo antibacterial assays in Galleria mellonella: PA2 shows potent anti MRSA activity and low toxicity*

We assessed the *in vivo* antibacterial activity of PA2 against MRSA JE2 using *G. mellonella* animal model and the results are presented in Fig. 7B. PA2 was selected for these studies due to its great antibacterial activity and low rate of resistance. First, we determined the *in vivo* toxicity of PA2 at different concentrations. Animals treated with PA2 at 75 mg/kg body weight have shown 100% survival after 4 days and animals treated with PA2 at 125 and 150 mg/kg body weight have shown 80% survival after 4 days indicating low *in vivo* toxicity of this peptide. These results are included in the supporting information SI10. After determining the safe doses of PA2, we evaluated the antibacterial *in vivo* activity of PA2 in animals infected with MRSA. PA2 displayed great antibacterial *in vivo* activity with 60% survival after 4 days with a single dose treatment of PA2 at 75 mg/kg body weight. Vancomycin displayed about 30% of survival after 4 days. These results indicate that PA2 is more effective than vancomycin to treat MRSA infections in this animal model.

## 4. Conclusion

In this work, we designed a small library of PAs and evaluated their antibacterial activity against gram-positive and gram-negative strains. Our findings indicate that the cationic charges, hydrophobicity morphology and stability of the self-assembled nanostructures play an important role in the antibacterial activity of these compounds. The toxicity of these compounds in red blood cells has been shown to be related with hydrophobicity and charge and it seems to be a very short window of hydrophobicity and charge balance that leads to low toxicity. PA1 demonstrated a very low antibacterial activity alone but it was able to potentiate the activity of Vancomycin with E. coli by a cooperative mechanism that leads to increased inner membrane permeability. This drug combination approach is a very promising approach to overcome the toxicity of PAs since sub-MIC concentrations are required for activity. In addition, PA2 and PA3 have shown potent broad-spectrum antibacterial activity against the strains tested. PA2 was the best candidate in this study showing low development of bacterial resistance and great *in vivo* activity. These findings are promising and open opportunities to further study the mechanism of action of drug combinations and the development of novel antibacterial PAs to overcome bacteria resistance.

## Declaration of Competing Interest

The authors declare that they have no known competing financial interests or personal relationships that could have appeared to influence the work reported in this paper.

## Data availability

Data will be made available on request.

## Acknowledge and Funding

This work was supported by Start-up funds (Depts. of Chemistry and Biology at UNO) and Fund for Undergraduate Scholarly Experience (UNO-FUSE). MC-S acknowledges support from the National Science Foundation (NSF), United States. CAREER Award (DMR-1941731). We would like to thank Alex Wu for helping with the synthesis of 3 PAs reported in this manuscript. The authors thank the Electron Microscopy

Core Facility (Tom Bargar and Nicholas Conoan) and Center for Drug Delivery and Nanomedicine (Svetlana G Romanova and Pratiksha Kakalij) at UNMC for experimental assistance. The authors further appreciate Luana J. de Campos at UNMC for helping with the antibacterial in *vivo* assays in *G. mellonella*. The authors also thank the American Red Cross for supplying blood products for this study.

## Appendix A. Supplementary data

Supplementary data to this article can be found online at https://doi.org/10.1016/j.bmc.2023.117481.

## References

1 CDC. COVID-19: U.S. Impact on antimicrobial resistance, Special Report 2022. Atlanta, GA: U.S. Department of Health and Human Services, CDC; 2022.
2 CDC. Antibiotic resistance threats in the United States, 2019. Atlanta, GA: U.S. Department of Health and Human Services, CDC; 2019.
3 2019 Antibacterial Agents in Clinical Development: An Analysis of the Antibacterial Clinical Development Pipeline. Geneva: World Health Organization; 2019. Licence: CC BY-NC-SA 3.0 IGO.
4 2021 Antibacterial Agents in Clinical and Preclinical Development: An Overview and Analysis. Geneva: World Health Organization; 2022. Licence: CC BY-NC-SA 3.0 IGO.
5 Breijyeh Z, Jubeh B, Karaman R. Resistance of gram-negative bacteria to current antibacterial agents and approaches to resolve it. *Molecules*. 2020;25. https://doi.org/10.3390/molecules25061340.
6 Delcour AH. Outer membrane permeability and antibiotic resistance. *Biochim Biophys Acta (BBA) - Prot Proteom*. 2009;1794:808–816. https://doi.org/10.1016/j.bbapap.2008.11.005.
7 MacNair CR, Brown ED. Outer membrane disruption overcomes intrinsic, acquired, and spontaneous antibiotic resistance. *MBio*. 2020;11:e01615–e01620. https://doi.org/10.1128/mBio.01615-20.
8 Mielke M, Oltmanns P, Ross B, Rotter M, Schmithausen RM, Sonntag HG, Trautmann M. Antibiotic resistance: what is so special about multidrug-resistant gram-negative bacteria? GMS Hyg Infect Control. 2017 Apr 10;12:Doc05. 10.3205/Dgkh000290. PMID: 28451516; PMCID: PMC5388835.
9 Zeng D, Debabov D, Hartsell TL, et al. Approved glycopeptide antibacterial drugs: mechanism of action and resistance. *Cold Spring Harbor Perspect Med*. 2016 Dec 1;6: A026989. https://doi.org/10.1101/Cshperspect.A026989. PMID: 27663982; PMCID: PMC5131748.
10 Stokes JM, MacNair CR, Ilyas B, et al. Pentamidine sensitizes gram-negative pathogens to antibiotics and overcomes acquired colistin resistance. *Nat Microbiol*. 2017;2:17028. https://doi.org/10.1038/nmicrobiol.2017.28.
11 Zhou Y, Huang W, Lei E, et al. Cooperative membrane damage as a mechanism for pentamidine-antibiotic mutual sensitization. *ACS Chem Biol*. 2022;17:3178–3190. https://doi.org/10.1021/acschembio.2c00613.
12 Sands M, Kron MA, Brown RB. Pentamidine: a review. *Rev Infect Dis*. 1985;7: 625–6344. https://doi.org/10.1093/clinids/7.5.625.
13 Kuryshev YA, Ficker E, Wang L, et al. Pentamidine-induced long QT syndrome and block of hERG trafficking. *J Pharmacol Exp Ther*. 2005;312:316. https://doi.org/10.1124/jpet.104.073692.
14 Mohammed EHM, Lohan S, Ghaffari T, Gupta S, Tiwari RK, Parang K. Membrane-active cyclic amphiphilic peptides: broad-spectrum antibacterial activity alone and in combination with antibiotics. *J Med Chem*. 2022;65:15819–15839. https://doi.org/10.1021/acs.jmedchem.2c01469.
15 Zeng P, Xu C, Liu C, et al. Novo designed hexadecapeptides synergize glycopeptide antibiotics vancomycin and teicoplanin against pathogenic klebsiella pneumoniae via disruption of cell permeability and potential. *ACS Appl Bio Mater*. 2020;3: 1738–1752. https://doi.org/10.1021/acsabm.0c00044.
16 Mood EH, Goltermann L, Brolin C, et al. Antibiotic potentiation in multidrug-resistant gram-negative pathogenic bacteria by a synthetic peptidomimetic. *ACS Infect Dis*. 2021;7:2152–2163. https://doi.org/10.1021/acsinfecdis.1c00147.
17 Kang HK, Park J, Seo CH, Park Y. PEP27-2, a potent antimicrobial cell-penetrating peptide, reduces skin abscess formation during *Staphylococcus aureus* infections in mouse when used in combination with antibiotics. *ACS Infect Dis*. 2021;7: 2620–2636. https://doi.org/10.1021/acsinfecdis.0c00894.
18 Konai MM, Haldar J. Lysine-based small molecule sensitizes rifampicin and tetracycline against multidrug-resistant *Acinetobacter baumannii* and *Pseudomonas aeruginosa*. *ACS Infect Dis*. 2020;6:91–99. https://doi.org/10.1021/acsinfecdis.9b00221.
19 Shao Z, Wulandari E, Lin RCY, Xu J, Liang K, Wong EHH. Two plus One: combination therapy tri-systems involving two membrane-disrupting antimicrobial macromolecules and antibiotics. *ACS Infect Dis*. 2022;8:1480–1490. https://doi.org/10.1021/acsinfecdis.2c00087.
20 Namivandi-Zangeneh R, Sadrearhami Z, Dutta D, Willcox M, Wong EHH, Boyer C. Synergy between synthetic antimicrobial polymer and antibiotics: a promising platform to combat multidrug-resistant bacteria. *ACS Infect Dis*. 2019;5:1357–1365. https://doi.org/10.1021/acsinfecdis.9b00049.
21 Mahlapuu M, Håkansson J, Ringstad L, Björn C. Antimicrobial peptides: an emerging category of therapeutic agents. *Front Cell Infect Microbiol*. 2016;6.
22 Ding Y, Ting JP, Liu J, Al-Azzam S, Pandya P, Afshar S. Impact of non-proteinogenic amino acids in the discovery and development of peptide therapeutics. *Amino Acids*. 2020;52:1207–1226. https://doi.org/10.1007/s00726-020-02890-9.
23 Hamley IW. Lipopeptides: from self-assembly to bioactivity. *Chem Commun*. 2015;51: 8574–8583. https://doi.org/10.1039/C5CC01535A.
24 Zhang Q-Y, Yan Z-B, Meng Y-M, et al. Antimicrobial peptides: mechanism of action, activity and clinical potential. *Mil Med Res*. 2021;8:48. https://doi.org/10.1186/s40779-021-00343-2.
25 Huan Y, Kong Q, Mou H, Yi H. Antimicrobial peptides: classification, design, application and research progress in multiple fields. *Front Microbiol*. 2020;11.
26 Rosenfeld Y, Lev N, Shai Y. Effect of the hydrophobicity to net positive charge ratio on antibacterial and anti-endotoxin activities of structurally similar antimicrobial peptides. *Biochemistry*. 2010;49:853–861. https://doi.org/10.1021/bi900724x.
27 Rodrigues de Almeida N, Han Y, Perez J, Kirkpatrick S, Wang Y, Sheridan MC. Design, synthesis, and nanostructure-dependent antibacterial activity of cationic peptide amphiphiles. *ACS Appl Mater Interfaces*. 2019;11:2790–2801. https://doi.org/10.1021/acsami.8b17808.
28 Conda-Sheridan M, Lee SS, Preslar AT, Stupp SI. Esterase-activated release of naproxen from supramolecular nanofibres. *Chem Commun*. 2014;50:13757–13760. https://doi.org/10.1039/C4CC06340F.
29 Zaldivar G, Vemulapalli S, Udumula V, Conda-Sheridan M, Tagliazucchi M. Self-assembled nanostructures of peptide amphiphiles: charge regulation by size regulation. *J Phys Chem C*. 2019;123:17606–17615. https://doi.org/10.1021/acs.jpcc.9b04280.
30 Ye M, Zhao Y, Wang Y, et al. A dual-responsive antibiotic-loaded nanoparticle specifically binds pathogens and overcomes antimicrobial-resistant infections. *Adv Mater*. 2021;33:2006772. https://doi.org/10.1002/adma.202006772.
31 Blaskovich MAT, Kavanagh AM, Elliott AG, et al. The antimicrobial potential of cannabidiol. *Commun Biol*. 2021;4:7. https://doi.org/10.1038/s42003-020-01530-y.
32 Ma Z, Kim D, Adesogan AT, Ko S, Galvao K, Jeong KC. Chitosan microparticles exert broad-spectrum antimicrobial activity against antibiotic-resistant micro-organisms without increasing resistance. *ACS Appl Mater Interfaces*. 2016;8:10700–10709. https://doi.org/10.1021/acsami.6b00894.
33 Ignasiak K, Maxwell A. *Galleria mellonella* (greater wax moth) larvae as a model for antibiotic susceptibility testing and acute toxicity trials. *BMC Res Notes*. 2017;10:428. https://doi.org/10.1186/s13104-017-2757-8.
34 Li L, Vorobyov I, Allen TW. The different interactions of lysine and arginine side chains with lipid membranes. *J Phys Chem B*. 2013;117:11906–11920. https://doi.org/10.1021/jp405418y.
35 Dong N, Wang C, Zhang T, et al. Bioactivity and bactericidal mechanism of histidine-rich β-hairpin peptide against gram-negative bacteria. *Int J Mol Sci*. 2019;20. https://doi.org/10.3390/ijms20163954.
36 Bi X, Wang C, Dong W, Zhu W, Shang D. Antimicrobial properties and interaction of two Trp-substituted cationic antimicrobial peptides with a lipid bilayer. *J Antibiot*. 2014;67:361–368. https://doi.org/10.1038/ja.2014.4.
37 Isom DG, Castañeda CA, Cannon BR, García-Moreno EB. Large shifts in pKa values of lysine residues buried inside a protein. *Proc Natl Acad Sci*. 2011;108:5260–5265. https://doi.org/10.1073/pnas.1010750108.
38 Cote Y, Fu IW, Dobson ET, Goldberger JE, Nguyen HD, Shen JK. Mechanism of the pH-controlled self-assembly of nanofibers from peptide amphiphiles. *J Phys Chem C*. 2014;118:16272–16278. https://doi.org/10.1021/jp5048024.
39 Cui H, Webber MJ, Stupp SI. Self-assembly of peptide amphiphiles: from molecules to nanostructures to biomaterials. *Pept Sci*. 2010;94:1–18. https://doi.org/10.1002/bip.21328.
40 Hendricks MP, Sato K, Palmer LC, Stupp SI. Supramolecular assembly of peptide amphiphiles. *Acc Chem Res*. 2017;50:2440–2448. https://doi.org/10.1021/acs.accounts.7b00297.
41 Paramonov SE, Jun H-W, Hartgerink JD. Self-assembly of peptide−amphiphile nanofibers: the roles of hydrogen bonding and amphiphilic packing. *J Am Chem Soc*. 2006;128:7291–7298. https://doi.org/10.1021/ja060573x.
42 Boothroyd S, Saiani A, Miller AF. Controlling network topology and mechanical properties of co-assembling peptide hydrogels. *Biopolymers*. 2014;101:669–680. https://doi.org/10.1002/bip.22435.
43 Chen Y, Gan HX, Tong YW. pH-controlled hierarchical self-assembly of peptide amphiphile. *Macromolecules*. 2015;48:2647–2653. https://doi.org/10.1021/ma502572w.
44 Selvamani V. Chapter 15 - Stability studies on nanomaterials used in drugs. In: Mohapatra SS, Ranjan S, Dasgupta N, Mishra RK, Thomas S, editors. Characterization and biology of nanomaterials for drug delivery. Elsevier; 2019. p. 425–4. 10.1016/B978-0-12-814031-4.00015-5.
45 Yang L, Chen C, Liang T, et al. Disassembling ability of lipopeptide promotes the antibacterial activity. *J Colloid Interface Sci*. 2023. https://doi.org/10.1016/j.jcis.2023.05.168.
46 Chaudhury S, Ripoll DR, Wallqvist A. Structure-based pKa prediction provides a thermodynamic basis for the role of histidines in pH-induced conformational transitions in dengue virus. *Biochem Biophys Rep*. 2015;4:375–385. https://doi.org/10.1016/j.bbrep.2015.10.014.
47 Kacprzyk L, Rydengård V, Mörgelin M, et al. Antimicrobial activity of histidine-rich peptides is dependent on acidic conditions. *Biochim Biophys Acta (BBA) - Biomembr*. 2007;1768:2667–2680. https://doi.org/10.1016/j.bbamem.2007.06.020.
48 Lan Y, Langlet-Bertin B, Abbate V, et al. Incorporation of 2,3-diaminopropionic acid into linear cationic amphipathic peptides produces pH-sensitive vectors. *Chembiochem*. 2010;11:1266–1272. https://doi.org/10.1002/cbic.201000073.
49 James Mason A, Claire Gasnier, Antoine Kichler, Gilles Prévost, Dominique Aunis, Marie-Hélène Metz-Boutigue, Burkhard Bechinger. Enhanced membrane disruption and antibiotic action against pathogenic bacteria by designed histidine-rich peptides

at acidic pH. Antimicrob Agents Chemother 2006;50(10):3305–11. 10.1128/AAC.00490-06.
50 Wang Z, Li Q, Li J, et al. pH-responsive antimicrobial peptide with selective killing activity for bacterial abscess therapy. *J Med Chem*. 2022;65:5355–5373. https://doi.org/10.1021/acs.jmedchem.1c01485.
51 Mant CT, Jiang Z, Gera L, et al. Novo designed amphipathic α-helical antimicrobial peptides incorporating Dab and Dap residues on the polar face to treat the gram-negative pathogen, *Acinetobacter baumannii*. *J. Med. Chem.* 2019;62:3354–3366. https://doi.org/10.1021/acs.jmedchem.8b01785.
52 Zelezetsky I, Pacor S, Pag U, et al. Controlled alteration of the shape and conformational stability of α-helical cell-lytic peptides: effect on mode of action and cell specificity. *Biochem J*. 2005;390:177–188. https://doi.org/10.1042/BJ20042138.
53 Uggerhøj LE, Poulsen TJ, Munk JK, et al. Rational design of alpha-helical antimicrobial peptides: do's and don'ts. *Chembiochem*. 2015;16:242–253. https://doi.org/10.1002/cbic.201402581.
54 Dong W, Mao X, Guan Y, Kang Y, Shang D. Antimicrobial and anti-inflammatory activities of three chensinin-1 peptides containing mutation of glycine and histidine residues. *Sci Rep*. 2017;7:40228. https://doi.org/10.1038/srep40228.
55 Hartmann GR, Heinrich P, Kollenda MC, Skrobranek B, Tropschug M, Weiß W. Molecular mechanism of action of the antibiotic rifampicin. *Angew Chem Int Ed Eng*. 1985;24:1009–1014. https://doi.org/10.1002/anie.198510093.
56 Odds FC. Synergy, antagonism, and what the chequerboard puts between them. *J Antimicrob Chemother*. 2003;52:1. https://doi.org/10.1093/jac/dkg301.
57 Schweizer L, Ramirez D, Schweizer F. Effects of lysine N-ζ-methylation in ultrashort tetrabasic lipopeptides (UTBLPs) on the potentiation of rifampicin, novobiocin, and niclosamide in gram-negative bacteria. *Antibiotics*. 2022:11 (3). https://doi.org/10.3390/antibiotics11030335.
58 Vaara M, Vaara T. Sensitization of gram-negative bacteria to antibiotics and complement by a nontoxic oligopeptide. *Nature*. 1983;303:526–528. https://doi.org/10.1038/303526a0.
59 Powers MJ, Trent MS. Expanding the paradigm for the outer membrane: *Acinetobacter baumannii* in the absence of endotoxin. *Mol Microbiol*. 2018;107:47–56. https://doi.org/10.1111/mmi.13872.
60 Vaara M. Agents that increase the permeability of the outer membrane. *Microbiol Rev*. 1992;56:395–411. https://doi.org/10.1128/mr.56.3.395-411.1992.
61 Lei E, Tao H, Jiao S, et al. Potentiation of vancomycin: creating cooperative membrane lysis through a "derivatization-for-sensitization" approach. *J Am Chem Soc*. 2022;144:10622–10639. https://doi.org/10.1021/jacs.2c03784.
62 Daniela Münch, Ina Engels, Anna Müller, Katrin Reder-Christ, Hildegard Falkenstein-Paul, Gabriele Bierbaum, Fabian Grein, Gerd Bendas, Hans-Georg Sahl, Tanja Schneider. Structural variations of the cell wall precursor lipid II and their influence on binding and activity of the lipoglycopeptide antibiotic oritavancin. Antimicrob Agents Chemother 2015;59(2):772–81. 10.1128/aac.02663-14.
63 Wang F, Zhou H, Olademehin OP, Kim SJ, Tao P. Insights into key interactions between vancomycin and bacterial cell wall structures. *ACS Omega*. 2018;3:37–45. https://doi.org/10.1021/acsomega.7b01483.
64 Zeng P, Xu C, et al. Novo designed hexadecapeptides synergize glycopeptide antibiotics vancomycin and teicoplanin against pathogenic klebsiella pneumoniae via disruption of cell permeability and potential. *ACS Appl. Bio Mater*. 2020;3:1738–1752. https://doi.org/10.1021/acsabm.0c00044.
65 Halder S, Yadav KK, Sarkar R, et al. Alteration of zeta potential and membrane permeability in bacteria: a study with cationic agents. *Springerplus*. 2015;4:672. https://doi.org/10.1186/s40064-015-1476-7.
66 Ferreyra Maillard APV, Espeche JC, Maturana P, Cutro AC, Hollmann A. Zeta potential beyond materials science: applications to bacterial systems and to the development of novel antimicrobials. *Biochim Biophys Acta (BBA) – Biomembr*. 2021;1863, 183597. https://doi.org/10.1016/j.bbamem.2021.183597.
67 Alves CS, Melo MN, Franquelim HG, et al. *Escherichia coli* cell surface perturbation and disruption induced by antimicrobial peptides BP100 and pepR *. *J Biol Chem*. 2010;285:27536–27544. https://doi.org/10.1074/jbc.M110.130955.
68 Grein F, Müller A, Scherer KM, et al. Ca2+-daptomycin targets cell wall biosynthesis by forming a tripartite complex with undecaprenyl-coupled intermediates and membrane lipids. *Nat Commun*. 2020;11:1455. https://doi.org/10.1038/s41467-020-15257-1.
69 Pérez-Peinado C, Dias SA, Domingues MM, et al. Mechanisms of bacterial membrane permeabilization by crotalicidin (Ctn) and its fragment Ctn(15–34), antimicrobial peptides from rattlesnake venom. *J Biol Chem*. 2018;293:1536–1549. https://doi.org/10.1074/jbc.RA117.000125.
70 Armas F, Pacor S, Ferrari E, et al. Design, antimicrobial activity and mechanism of action of Arg-rich ultra-short cationic lipopeptides. *PLoS One*. 2019;14:e0212447.
71 Heidary M, Khosravi AD, Khoshnood S, Nasiri MJ, Soleimani S, Goudarzi M. Daptomycin. *J Antimicrob Chemother*. 2018;73:1–11. https://doi.org/10.1093/jac/dkx349.
72 Greco I, Molchanova N, Holmedal E, et al. Correlation between hemolytic activity, cytotoxicity and systemic in vivo toxicity of synthetic antimicrobial peptides. *Sci Rep*. 2020;10:13206. https://doi.org/10.1038/s41598-020-69995-9.
73 Alves AC, Ribeiro D, Nunes C, Reis S. Biophysics in cancer: the relevance of drug-membrane interaction studies. *Biochim Biophys Acta (BBA) - Biomembr*. 2016;1858:2231–2244. https://doi.org/10.1016/j.bbamem.2016.06.025.